The Journal of Immunology

Dynamics of Macrophage Cell Populations During Murine Pulmonary Tuberculosis

Mercedes Gonzalez-Juarrero, Tae Sun Shim, Andre Kipnis, Ana Paula Junqueira-Kipnis and Ian M. Orme

J Immunol 2003; 171:3128-3135; ;
doi: 10.4049/jimmunol.171.6.3128
http://www.jimmunol.org/content/171/6/3128

The Journal of Immunology is published twice each month by
The American Association of Immunologists, Inc.,
1451 Rockville Pike, Suite 650, Rockville, MD 20852

Print ISSN: 0022-1767 Online ISSN: 1550-6606.

Dynamics of Macrophage Cell Populations During Murine Pulmonary Tuberculosis[1]

Mercedes Gonzalez-Juarrero,[2] Tae Sun Shim,[3] Andre Kipnis, Ana Paula Junqueira-Kipnis, and Ian M. Orme

The influx of macrophages into the lungs is the major component of the granulomatous response to infection with *Mycobacterium tuberculosis*. In this investigation we used flow cytometric analysis to define macrophage populations entering the airways and lung tissues of infected mice. We demonstrate that by the judicious use of cell surface markers, especially CD11b and CD11c, several cell populations can be distinguished, allowing cell sorting and morphological definition. Primary populations of $CD11b^{-}/CD11c^{+/high}$ were defined as alveolar macrophages, $CD11b^{high}/CD11c^{+/high}$ as dendritic cells, and $CD11b^{+/mid}/CD11c^{+/mid}$ as small macrophages or monocytes, and changes in the activation phenotype of these populations were followed over the early course of the infection. In further studies, these cell populations were compared with cells harvested during the chronic stage of the disease. During the chronic stage of infection, Ag-presenting class II molecules and activation markers were poorly expressed on dendritic, small macrophage, and monocyte cell populations, which may have important implications for the breakdown of the lesions during reactivation disease. This analytical approach may facilitate the further characterization of macrophage populations entering into the lung tissues and their relative contributions to host resistance to tuberculosis infection. *The Journal of Immunology*, 2003, 171: 3128–3135.

Pulmonary tuberculosis is caused by infection with *Mycobacterium tuberculosis*, and current estimates suggest that one-third of the world's population has been exposed. The majority of such people are probably able to eliminate the organism, but ~10% develop a chronic or latent state of infection that will last for the rest of their lives (1).

Macrophages, granulocytes, and dendritic cells in the lungs represent the first line of defense against pathogens entering the lungs. Among these, dendritic cells are clearly a key population because of their ability to transport and present Ags to naive T cells in the secondary lymphoid organs, thus initiating adaptive immunity (2, 3). In addition, other cells of the macrophage/monocyte lineage are recruited into the developing granuloma, where they surround the sites of infection and control and contain the surviving bacteria after receiving appropriate activating signals from Th1 CD4 T cells (4–7).

Just as the T cell response to tuberculosis is complex (7, 8), it is now apparent that the overall macrophage response is a dynamic event. To date, however, the kinetics of the macrophage response has not been clearly defined. The growing availability of Abs to macrophage cell surface markers, coupled with an improved understanding of how expression of these markers changes, particularly those expressed by dendritic cells, now allows a better definition of these events.

In the present study, flow cytometry was used to define the influx of cells into the lungs during the early stage of pulmonary *M. tuberculosis* infection. Based on expression of the cell surface markers, several distinct populations of macrophages, as well as granulocytes and NK cells, could be distinguished. In addition, maturation of incoming dendritic cells could be identified as the immune response to the infection developed. Interestingly, markers of activation on these cell populations that were evident during the early phase of the infection were observed to be lost at a much later time point when the lung infection is thought to be in some form of latent state (4). Taken together, the data show that during the course of pulmonary *M. tuberculosis* infection, there is activation of macrophages and dendritic cell populations during the early phase that are associated with development of an effective immune response; however, during the chronic phase of infection these cell populations were not activated and resulted in down-regulation of the immune response.

Materials and Methods

Mice

Specific pathogen-free female C57BL/6 mice (The Jackson Laboratory, Bar Harbor, ME) at 6–8 wk old were used. They were housed under barrier conditions in a level III biosafety facility and were allowed free access to sterile chow and water.

Experimental infections

M. tuberculosis, Erdman strain (TMCC 107), was grown from low-passage seed lots in Proskauer-Beck liquid medium containing 0.02% Tween 80 to mid-log phase, then aliquoted and frozen at −70°C until use. Mice were infected aerogenically with the Erdman strain of *M. tuberculosis* by using a Glas-Col aerosol generation device (Glass-Col, Terre Haute, IN) as previously described (9) to result in the deposition of ~200 bacilli within the lungs.

Mycobacteria Research Laboratories, Department of Microbiology, Immunology and Pathology, Colorado State University, Fort Collins, CO 80523

Received for publication April 4, 2003. Accepted for publication July 9, 2003.

The costs of publication of this article were defrayed in part by the payment of page charges. This article must therefore be hereby marked *advertisement* in accordance with 18 U.S.C. Section 1734 solely to indicate this fact.

[1] This work was supported by National Institutes of Health Grants AI-40488 and AI-44072 and by a Supplementary Award for Reentry into the Biomedical Sciences from the National Institute of Allergy and Infectious Diseases, National Institutes of Health (to M.G.-J.). A.K. was supported by the Conselho Nacional de Desenvolvimento Cientifico e Tecnologico, Brazil.

[2] Address correspondence and reprint requests to Dr. Mercedes Gonzalez-Juarrero, Mycobacteria Research Laboratories, Department of Microbiology, Immunology and Pathology, Colorado State University, 200 Lake Street, Fort Collins, CO 80523. E-mail address: malba@lamar.colostate.edu

[3] Current address: Division of Pulmonary and Critical Care Medicine, Department of Internal Medicine, University of Ulsan College of Medicine, Asan Medical Center, 388-1 Pungnap-dong, Songpa-gu, Seoul 138-600, South Korea.

0022-1767/03/$02.00

Preparation of bronchoalveolar lavage (BAL)[4] and lung cell suspensions

Mice were euthanized and the pulmonary cavities were opened. After severing the descending aorta, the blood in the lungs was cleared by perfusion through the right heart with 5 ml of PBS containing 50 U of heparin (Sigma-Aldrich, St. Louis, MO) per ml until the lungs became whitish. Using an 18-gauge needle, the trachea was cannulated, and ~1 ml of heparin/PBS was slowly injected into the lungs and then withdrawn. This procedure was repeated ~7–10 times, and a total of 5–8 ml of lavage fluid was collected.

To obtain lung cell populations, the lungs were perfused with heparin solution as above. Thereafter, they were aseptically removed and cut into small pieces. The dissected tissue was incubated in RPMI medium (RPMI 1640 (Life Technologies, Gaithersburg, MD) supplemented with 1% glutamine (Sigma-Aldrich), 0.1 mM nonessential amino acids (Life Technologies), 50 μM 2-ME (Sigma-Aldrich), and 1% penicillin-streptomycin (Sigma-Aldrich)) containing collagenase XI (0.7 mg/ml; Sigma-Aldrich) and type IV bovine pancreatic DNase (30 mg/ml; Sigma-Aldrich) during 30–45 min at 37°C. The action of the enzymes was stopped by adding 10 ml of RPMI medium containing 10% FBS (cRPMI), and digested lungs were further disrupted by gently pushing the tissue through a nylon screen (70 μm). The single-cell suspension was then washed and centrifuged at 200 × *g*. To lyse contaminating RBCs, the cell pellet was incubated during 5 min at room temperature with 5 ml of Gey's solution (NH_4Cl and $KHCO_3$). Cells were then washed with cRPMI and resuspended in 2 ml of cRPMI.

Single-cell suspensions obtained by enzymatic digestion as indicated above were washed in deficient RPMI (Irvine Scientific, Santa Ana, CA), which was supplemented with 1% L-glutamine (Sigma-Aldrich), 1% HEPES (Sigma-Aldrich), 0.1% sodium azide (N_3Na; Sigma-Aldrich), and 2% FBS. The cells were stained during 30 min at 4°C with directly conjugated Abs. mAbs specific for CD11c (clone HL3, hamster IgG1), CD11b (Mac-1, clone M1/70, rat IgG2a), Gr-1 (clone RB6-8C5, rat IgG2b), CD3e (clone 145-2C11, hamster IgG1), CD45RB/B220 (clone RA3-6B2, rat IgG2a), NK-1.1 (clone PK136, mouse IgG2a), CD16/CD32 (clone 2.4G2, rat IgG2b), CD40 (clone 3-23, rat IgG2a), CD80 (clone 16-10A1, hamster IgG), CD86 (clone GL1, rat IgG2a), I-A/I-E MHC class II Ag (clone 2G9, rat IgG2a), rat IgG2a, rat IgG2b, rat IgG1, mouse IgG2a, and hamster IgG were purchased from BD PharMingen (San Diego, CA) or eBioscience (San Diego, CA) as direct conjugates to FITC, PE, PerCP, PerCP-cyanine 5.5 (PerCP-Cy5.5), or allophycocyanin. Purified rat anti-mouse CD16/CD32 mAb (mouse Fc-Block) was also purchased from BD PharMingen and used to prevent nonspecific binding of Abs to the Fc receptors. mAb F4/80 (clone CI:A3-1, rat IgG2b) as a direct conjugate to FITC was purchased from Serotec (Raleigh, NC). Cell acquisition was performed with a dual-laser flow cytometer (FACSCalibur; BD Biosciences, Mountain View, CA). Compensation of the spectral overlap for each fluorochrome was done gating in the R3 region and using CD11b Ag. The data were analyzed using CellQuest software (BD Biosciences).

Cell sorting

The lungs were enzymatically digested as indicated above, and the single cell suspension obtained was labeled with FITC-conjugated CD11b and PE-conjugated CD11c Abs. Lymphocytes and macrophages were gated according to their sizes and granularity defined in the forward light scatter (FSC) and side light scatter (SSC) plot. Cell populations were sorted based on their CD11b/CD11c profiles using a MoFlo flow cytometer/cell sorter (DakoCytomation, Fort Collins, CO). The $CD11b^-$/ $CD11c^{+/high}$, $CD11b^+/CD11c^{+/high}$, $CD11b^{+/high}/CD11c^-$, $CD11b^{+/mid}/CD11c^-$, and $CD11b^{+/mid}/CD11c^{+/low}$ cell populations in macrophage area (R3) were sorted and, in the same manner, the $CD11b^{+/low}/CD11c^-$ and $CD11b^{+/mid}/CD11c^-$ cells were also sorted in the lymphocyte area (R2). To obtain higher purity of cell population, an enrichment mode was performed previously to the purified mode sort.

Cell morphology and microscopic examination

Sorted cell suspensions were cytospun onto glass slides (Shandon Instruments, Sewickley, PA) and were stained using the Hema 3 stain set (Biochemical Science, Swedesboro, NJ). Cell morphology was determined by microscopic examination.

[4] Abbreviations used in this paper: BAL, bronchoalveolar lavage; FSC, forward light scatter; SSC, side light scatter; MFC, mean fluorescence channel.

Results

Early influx of cells into the bronchoalveolar space after M. tuberculosis *infection*

Cells in the BAL fluid from naive mice and mice challenged 21 days previously with *M. tuberculosis* (Fig. 1) were analyzed according to their FSC and SSC characteristics by flow cytometry as well as for their expression of CD11b and CD11c (Figs. 1 and 2). Cells that clustered as FCS^{low}/SSC^{low} were gated as regions R1 and R2 and were found to be mainly $CD3^+$ (Figs. 2 and 3). Cells defined as FSC^{high}/SSC^{high} were gated as R3 and were shown to be $CD11b^-/CD11c^+$ (Fig. 1). Most cells (90–95%) in the BAL fluid from naive mice had this latter expression pattern and had typical morphology of macrophages and immature dendritic cells (data not shown). Cells in Fig. 1*B* defined as $CD11b^+/CD11c^-$ were also positive for Gr-1 expression (Fig. 1*C*), indicating that they were granulocytes.

The total number of cells obtained in the BAL from mice infected with a low-dose aerosol of *M. tuberculosis* increased as the infection progressed (Table I). Cells were analyzed by their FSC/SSC profile at 3, 14, and 21 days postchallenge and were compared with the same regions obtained with BAL fluid from naive mice. The number of cells in the lymphocyte gate (R2) increased steadily from day 3 to day 21 of the infection (Table I). As above, cell populations within the R3 region were differentiated according to their CD11b/CD11c profiles. There were increased numbers of $CD11b^+/CD11c^+$ cells over the first 21 days of the infection, as well as increases in Gr-1^+ $CD11b^+/CD11c^-$ cells (Fig. 1*C* and Table I).

Definition of lung macrophage populations from naive mice

Similar flow cytometric studies were performed using cells released from the lung tissues by enzymatic digestion. The FSC/SSC profile of these cells from naive mice resolved into two dense cell populations: an $FSC^{low-mid}/SSC^{low}$ area (R1 and R2) and cells that were $FSC^{mid-high}/SSC^{mid-high}$, designated region R3 (Fig. 2*A*). As above, $CD11c^+$ alveolar macrophages obtained by this method were located in R3 (Fig. 2).

The $FSC^{low-mid}/SSC^{low}$ region of lung cells from naive mice was further subdivided into R1 and R2 regions (Fig. 2*A*, *left* and

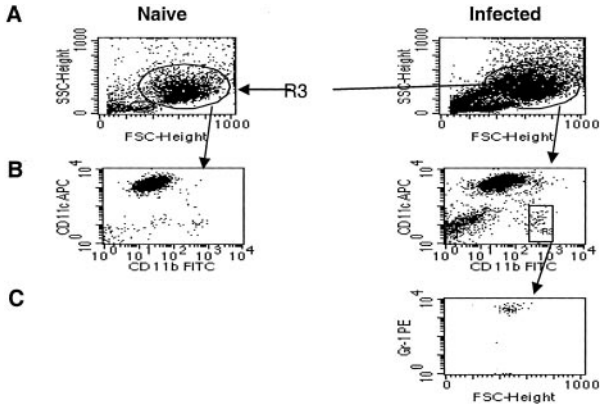

FIGURE 1. FSC/SSC (*A*), CD11b/CD11c (*B*), and FSC/Gr-1 (*C*) dot plots of cells from BAL before and 21 days after infection with *M. tuberculosis*. *A*, Cells from BAL fluid of naive mice and *M. tuberculosis*-infected mice. Cells defined as FSC^{low}/SSC^{low} were gated as R2, and cells defined as $FSC^{mid-high}/SSC^{mid-high}$ were gated as R3. *B*, Cells from BAL fluid of naive and *M. tuberculosis*-infected mice at 21 days postchallenge. After infection, there is an increase of the $CD11b^+/CD11c^+$ and $CD11b^+/CD11c^-$ cells. *C*, The $CD11b^+/CD11c^-$ cell population from *B* was further characterized as Gr-1^+ and, therefore, granulocytes.

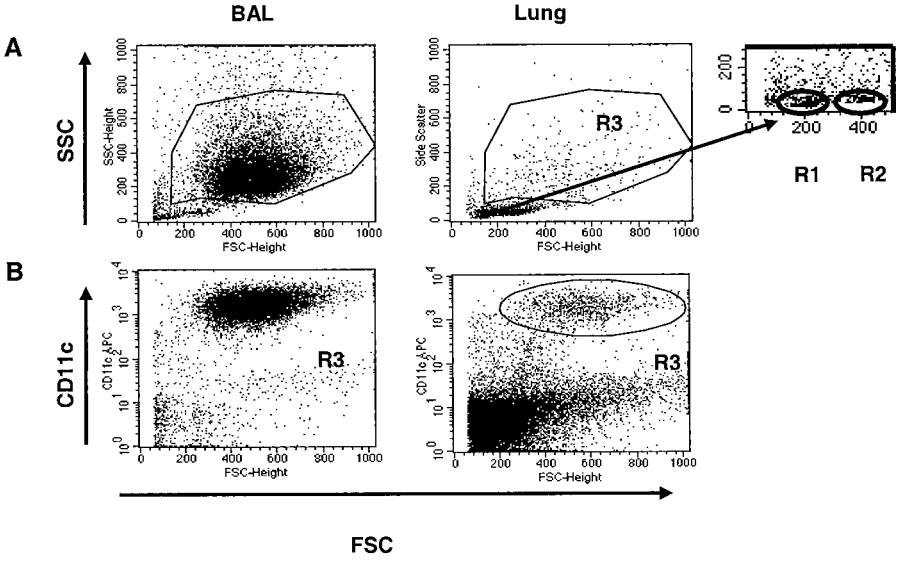

FIGURE 2. Comparative analysis of the FSC/SSC and CD11c expression of cells from BAL fluid and lung digested cells of naive mice. Cells from BAL fluid or lung cell suspension were gated in regions R1, R2, and R3 (*A*), and expression of CD11c marker for region R3 from each cell suspension was analyzed (*B*). Most cells in the BAL fluid were found in R3 and were positive for CD11c Ag. Also, cells in the R3 gate from lung-digested cells were CD11c positive.

right, respectively). In the R2 area, cells were $CD3^+$ (42%; Fig. 3*A*), $NK1.1^+$ (8%; Fig.3*B*), or $B220^+$ (33%; data not shown). Only a few $Gr\text{-}1^+$ cells (0.9%) were located in the R2 area (data not shown). Approximately 23% of cells in the R2 region stained positive for $CD11b^+$ (Fig. 3*A*), and among those 8% were $NK1.1^+/CD11b^{low}$ and another 8% were $NK1.1^-/CD11b^{+/high}$ (Fig. 3*B*). Furthermore, $CD11b^+$ cells in the R2 region could be subdivided into $NK1.1^+$ and $NK1.1^-$ cells (Fig. 3*B*). The $CD11b^+/NK1.1^+$ were further characterized as lacking expression of F4/80 and were $CD11c^{+/low}$ (Fig. 3*B*, *panels 1* and *2*). In contrast, $CD11b^+/NK1.1^-$ cells were $F4/80^{+/mid}$ and $CD11c^-$ or $CD11c^{+/mid}$ (Fig. 3*B*, *panels 3* and *4*).

Cells in the R3 region could be separated into six distinct cell populations according to their expression of CD11b and CD11c (Fig. 4, *A* and *C*). These populations comprised of $CD11b^-/CD11c^{+/high}$ cells (R5), $CD11b^+/CD11c^{+/high}$ (R6), $CD11b^{+/mid}/CD11c^{+/mid}$ (R7), $CD11b^{+/mid}/CD11c^-$ (R8), $CD11b^{+high}/CD11c^-$ (R9), and $CD11b^-/CD11c^-$ (Fig. 4, *A* and *C*)

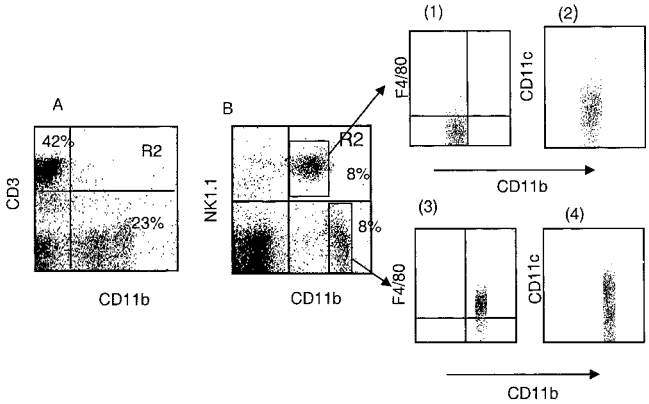

FIGURE 3. CD11b expression in cells of FSC^{low}/SSC^{low} or R2 gate were positive for CD11b expression. Cells from lung-digested tissue gated in R2 as indicated in Fig. 2, and analysis for expression of cell marker such as CD11b and F4/80 is known to be characteristic of the macrophage lineage cells. *A*, Cells in R2 were analyzed for CD3 and CD11b expression. *B*, Cells in R2 were analyzed for CD11b and NK1.1 and were further characterized for F4/80 and CD11c expression (*panels 1–4*).

Cell sorting and microscopic examination

Phenotypic characterization of lung cell populations by flow cytometry was used to conduct high-speed cell sorting of each population and further examination of morphology by microscopy. The dot plots for each sorted population are shown in Fig. 5. The percentage of positive cells in the CD11b/CD11c dot plot and the purity obtained after sorting each cell population were 9% positive and 91% purity for $CD11b^-/CD11c^{+/high}$ (R5), 1% and 56% for $CD11b^+/CD11c^{+/high}$ (R6), 3% and 62% for $CD11b^{+/mid}/CD11c^{+/mid}$ (R7), 6% and 88% for $CD11b^{+/mid}/CD11c^-$ (R8), and 2% and 85% for $CD11b^{+/high}/CD11c^-$ (R9), respectively. The morphology of the cells in the R5 gate was that of alveolar macrophages, and these were identical with cells obtained in the BAL fluid. This R5 region also contained some small veiled cells that resembled immature dendritic cells in this sorted population. Most cells sorted from the R6 region had morphology typical of dendritic cells, with large lateral nuclei and very long cytoplasmic processes. Sorted cells from R6 also contained some neutrophils characterized by multilobed nuclei. Cells in R7 and R8 were smaller cells in comparison with those in R5 and R6 and had the morphology of monocytes, with typical horseshoe-like nuclei or small macrophages. Cells in the R9 region were neutrophils with the same morphology as indicated above (Fig.5).

Changes in the phenotype and composition of lung macrophage cell populations during early stages of pulmonary M. tuberculosis *infection*

Changes in the phenotype and composition of cells in the lung were monitored from day 3 to day 21 after pulmonary challenge with *M. tuberculosis*. Cells in the R2 region were composed mainly of lymphocytes and monocytes, and these increased in number over this period of time as reported previously (10).

As indicated above, cells in the R3 region could be separated into six distinct cell populations according to their expression of CD11b and CD11c (Fig. 4). Fig. 4 compares the CD11b/CD11c profile from naive cells and cells harvested during the early stage (21 days) of the infection. The total number of cells defined as $CD11b^-/CD11c^{+/high}$ (R5), $CD11b^+/CD11c^{+/high}$ (R6), and $CD11b^{+/mid}/CD11c^{+/mid}$ (R7) increased as a result of the infection (Fig. 4, *A* and *B*).

Table I. *Cell composition in the BAL fluid during early phase of pulmonary infection with* M. tuberculosis[a]

	Days Postchallenge		
	3	14	21
Total number of cells ($\times 10^4$)*			27 ± 0.3
			77 ± 2.2
$CD3^+$ ($\times 10^4$)* (R2)	1.1 ± 0.43	1.15 ± 0.31	1.50 ± 0.48
	2.32 ± 0.16	**3.56 ± 1.31**	**19.0 ± 2.5**
$CD11b^+/CD11c^+$ ($\times 10^4$)* (R3)			0.60 ± 0.23
			4.04 ± 0.66
$CD11b^+/CD11c^-$ ($\times 10^4$) (R3)			8.6 ± 6.3
			8.3 ± 1.7
Gr-1^+ ($\times 10^4$)* (R3)			0.04 ± 0.05
			0.88 ± 0.16

[a] The average and SD from total numbers of cells, $CD3^+$, $CD11b^+/CD11c^+$, CD11b/$CD11c^-$, or GR-1^+ as defined in Fig. 1 were determined for cells in BAL fluid from naive (upper number) or infected mice (lower number in bold type).
*, $p < 0.05$ compared between naive and infected mice (Mann-Whitney *U* test).

Increased expression of costimulatory and activation surface molecules on macrophage cell populations during the early stage of infection with M. tuberculosis.

Macrophages, monocytes, and dendritic cells have different constitutive levels of costimulatory and activation markers. It is well established that differentiated naive dendritic cells are the most efficient APCs, in contrast with macrophages and monocytes, because they constitutively express high levels of costimulatory molecules (CD80 and CD86), CD40, and class II MHC Ags on their cell surface (2, 3). Therefore, from the CD11b/CD11c dot plot shown in Fig.4*C*, we analyzed differential expression of CD80, CD86, CD40, and class II MHC Ags on the surfaces of the cells in each region. Cells in regions R5, R6, R7, R8, and R9 were gated, and the mean fluorescence channel (MFC) for each marker was compared with the MFC from the other regions (Table II). As shown, the R6 region, which contained $CD11b^{+/high}/CD11c^{+/high}$ dendritic cells, had the highest constitutive expression of CD86, class II MHC, and CD40 Ags. CD80 Ag expression on cells within the naive population was similar on cells in regions R5 and R6. In addition, the $CD11b^{+/mid}/CD11c^-$ (R8) cells gated from the R3 region were F4/80 positive (data not shown). The cells in R9 gate and ~20% of cells in the R6 gate expressed Gr-1, were negative for costimulatory Ags, and had morphology typical of granulocytes (Fig. 5).

One of the earliest events upon Ag uptake and activation by dendritic cells is the up-regulation of costimulatory (CD80 and CD86) and activation markers such as MHC class II and CD40 Ag expression on their cell surfaces. Changes in these markers after infection are shown in Table II. Even by day 7 expression shifts were evident, with $CD11b^+/CD11c^{+/high}$ cells in region R6 increasing expression of CD86, CD40. Thus, MFC for CD86 at 7 days postchallenge increased from 356 to 696 in the R6 from naive and infected populations, respectively. In addition, the MFC for CD40 Ag expression for the same populations changed from 232 to 350. By 21 days postchallenge, there were major increases in CD80, CD86, MHC class II, and CD40 on cells in the R6 gate. The MFCs for CD86, CD40, and class II MHC Ags were also increased in R5, R7, and R8 (Table II and Fig. 6).

Changes in the numbers of macrophage cell populations during the early and chronic phase of the disease process

Table III shows the changes in the percentages of cells for each cytometric gating region at a time point well into the chronic or latent stage of the disease, compared with the early response. The percentage of alveolar macrophages in region R5, defined as $CD11b^-/CD11c^+$, decreased from 20% in naive mice to 16% and 6% during the early or chronic stage of infection, respectively. In contrast, dendritic cells in R6 defined as $CD11b^{+/high}/CD11c^{+/high}$

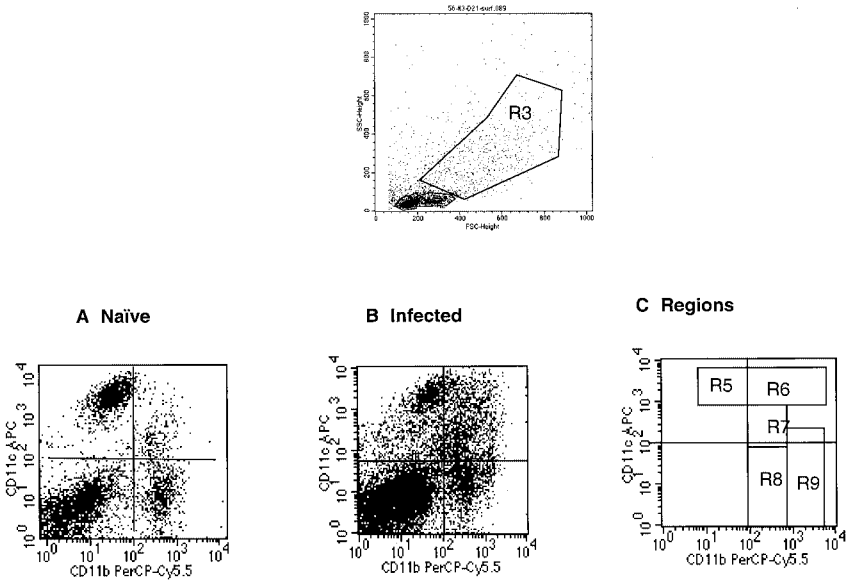

FIGURE 4. CD11b/CD11c dot plot of lung-digested cells. Lung cells gated in R3 stained for the CD11b and CD11c markers before (*A*) and 21 days after infection (*B*). The CD11b/CD11c dot plot was gated in five regions (*C*), namely $CD11b^-/CD11c^{+/high}$ (R5), $CD11b^+/CD11c^{+/high}$ (R6), $CD11b^{+/mid}/CD11c^{+/low}$ (R7), $CD11b^{+/mid}/CD11c^-$ (R8), and $CD11b^{+/high}/CD11c^-$ (R9).

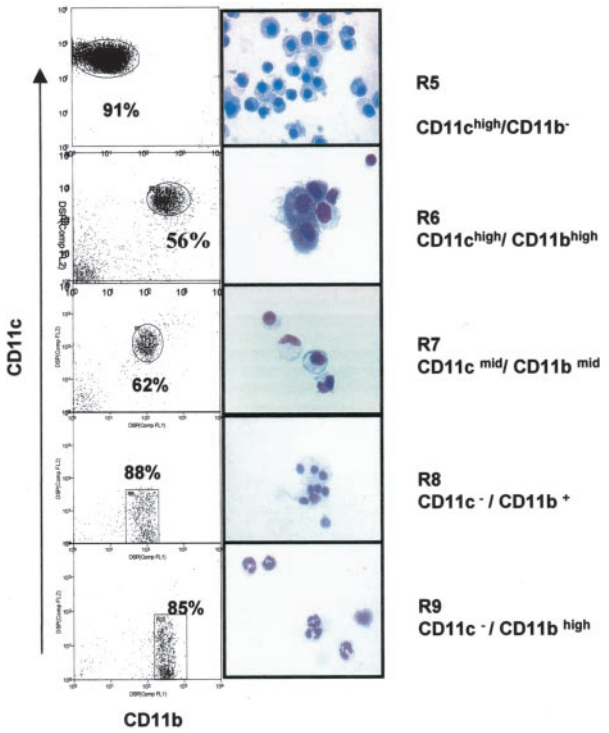

FIGURE 5. CD11b/CD11c dot plots of sorted lung cells. Cell populations were sorted based on their CD11b/CD11c profiles using a MoFlo flow cytometer/cell sorter (DAKO Cytomation, Fort Collins, CO). To obtain higher purity of cell population, an enrichment mode was performed before the purified mode sort. The *left panel* corresponds to dot plots of sorted cells from each region of the CD11b/CD11c profile. From the CD11b/CD11c dot plot were gated five regions, namely $CD11b^{-}/CD11c^{+/high}$ (R5), $CD11b^{+}/CD11c^{+/high}$ (R6), $CD11b^{+/mid}/CD11c^{+/low}$ (R7), $CD11b^{+/mid}/CD11c^{-}$ (R8), and $CD11b^{+/high}/CD11c^{-}$ (R9). The given number in each plot corresponds to the percentage of positive cells for each region sorted and is indicative of the purity obtained after each sort. The *right panel* corresponds to photomicrographs of Hema 3 stained, sorted and cytospun cells from each region of the CD11b/CD11c dot plot. The R5 and R9 show typical morphology of alveolar macrophages and granulocytes, respectively. The R6 consists of macrophages, dendritic cells, and some granulocytes. The R7 and R8 show a mixture of small macrophages and monocytes.

increased from 1% in naive to 7% and 4% during the early or chronic stage of infection, respectively. Monocytes and small macrophages in R7 defined as $CD11b^{+/mid}/CD11c^{+/mid}$ increased about twofold as a result of infection, as did cells in R8. Neutrophils in R9 increased from 4% in the early infection to 14% during the chronic phase, consistent with increasing lung damage occurring at this time (11).

Changes in costimulatory and activation markers in cells harvested during early and chronic infection

Fig. 6 shows the relative up-regulation for each cell population in the CD11b/CD11c dot plot for CD86, CD80, CD40, and class II MHC Ags during the course of the infection with *M. tuberculosis*. The ratio between the average of MFCs ($n = 4$) for each of these Ags on the defined cell populations from the early stage and those for cells harvested during chronic stage of infection was determined vs the naive population, respectively. As shown in Fig. 6, the ratio for each Ag (except CD80) was higher during the early phase, as would be anticipated. In contrast, ratios of ~1:1 were seen on cells harvested during the chronic phase, indicating that dendritic cells and macrophages present at this time were less activated and were not expressing MHC molecules at levels higher than that seen in age-matched naive controls.

Discussion

The results of this study show that the influx of macrophage populations into the developing granulomatous response in the lungs to pulmonary tuberculosis infection can be defined in six distinct populations based on the expression of the CD11b and CD11c cell surface markers. Each population had distinct morphological features that could be defined as alveolar macrophages, dendritic cells, monocytes, small macrophages, and granulocytes by analysis of the differential expression of CD11b and CD11c Ag expression on these cell populations. The kinetics of influx of monocytes into the lungs could be followed during infection, as well as their activation and potential differentiation into mature macrophage populations. Cells with both cell surface markers and morphology indicating dendritic cells could also be clearly defined. Interestingly, characteristic activation profiles seen on both these cells and other macrophage populations during the early phase of the infection were clearly modulated and reduced on similar cells harvested during the chronic phase of the disease, an observation that may have important consequences in terms of the development of reactivation disease.

Changes in surface expression of CD11b and CD11c allow some speculation as to the differentiation pathways of macrophages entering the lungs in response to the infection. The data suggest that $CD11b^{+/mid}/CD11c^{-}$ monocytes are recruited into the

Table II. *Flow cytometric comparison of the costimulatory and activation markers of lung cells between naive and 21 days post-*M. tuberculosis*-infected mice*[a]

Regions	Cells	MFC			
		CD86	CD40	MHC Class II	CD80
$CD11b^{-}/CD11c^{+/high}$ (R5)	Alveolar macrophages	63	21	319	124
		112	**35**	**2494**	**128**
$CD11b^{+/high}/CD11c^{+/high}$ (R6)	Dendritic cells	119	60	4108	136
		267	**406**	**6606**	**144**
$CD11b^{+/mid}/CD11c^{+/mid}$ (R7)	Monocytes and small macrophages	45	25	1283	28
		95	**83**	**2305**	**18**
$CD11b^{+/mid}/CD11c^{-}$ (R8)	Monocytes and small macrophages	41	9	161	7
		52	**31**	**756**	**8**
$CD11b^{+/high}/CD11c^{-}$ (R9)	Granulocytes	23	15	264	6
		30	**12**	**503**	**6**

[a] Lung cells were stained for the CD11b and CD11c markers. From the CD11b/CD11c dot plot were gated five regions, namely $CD11b^{-}/CD11c^{+/high}$ (R5), $CD11b^{+}/CD11c^{+/high}$ (R6), $CD11b^{+/mid}/CD11c^{+/low}$ (R7), $CD11b^{+/mid}/CD11c^{-}$ (R8), and $CD11b^{+/high}/CD11c^{-}$ (R9). Each region was further analyzed for expression of CD86, CD40, MHC class II, and CD80 molecules. Comparison of the MFC from naive (top number) and infected (bold numbers) lung-digested tissue are shown.

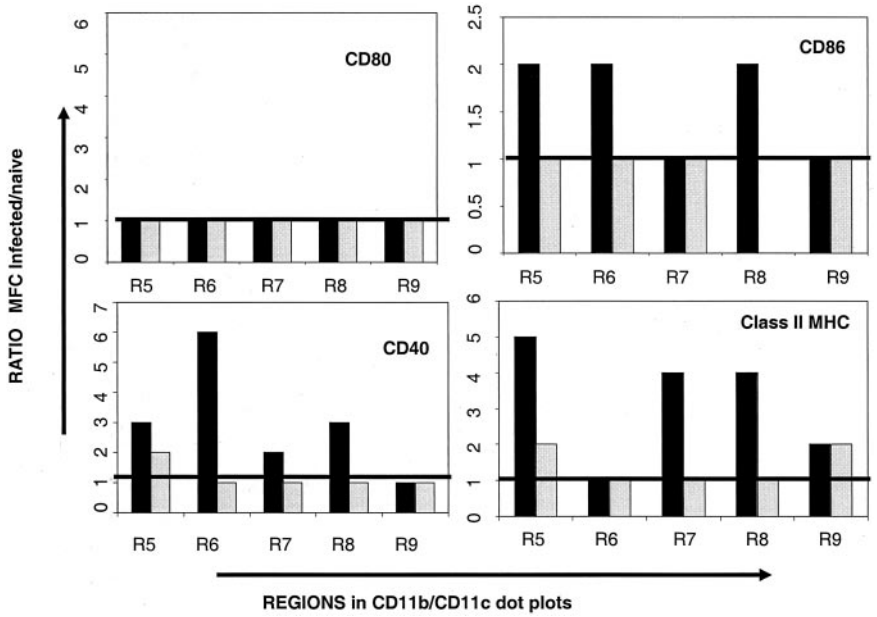

FIGURE 6. Comparative ratios of the MFCs for each Ag on lung cell populations from mice in early or chronic stage of infection vs naive. Comparative expression of CD80, CD86, CD40, and class II MHC Ags in each region of the CD11b/CD11c dot plot on lung cells from early or chronic stage of murine pulmonary infection with *M. tuberculosis* vs naive. Lung cells from mice in the naive ($n = 4$), early ($n = 4$), or chronic ($n = 4$) phase of infection after pulmonary challenge with *M. tuberculosis* were stained for CD11b and CD11c expression. First, from the CD11b/CD11c dot plot were gated five regions, namely alveolar macrophages $CD11b^{-}/CD11c^{+/high}$ (R5), dendritic cells $CD11b^{+}/CD11c^{+/high}$ (R6), monocytes and small macrophages $CD11b^{+/mid}/CD11c^{+/low}$ (R7), small macrophages $CD11b^{+/mid}/CD11c^{-}$ (R8), and neutrophils $CD11b^{+/high}/CD11c^{-}$ (R9). In addition, lung cells were also stained for CD80, CD86, CD40, and class II MHC expression. The average of the MFC from each group for each molecule in each region of the CD11b/CD11c dot plot was determined. Relative changes in expression of each molecule during the early or chronic phase of infection pulmonary challenge with *M. tuberculosis* were determined by the ratio of MFC obtained from cells from early (filled bars) or chronic (open bars) phase with the MFC obtained from naive cell populations. These results are from one representative experiment at each time point. Four experiments were done for early phase of infection (21 days) and two experiments were done for the chronic phase (240 days) of infection. Each experiment was done using naive mice of similar age.

lungs, where they increase their expression of CD11c and become $CD11b^{+/mid}/CD11c^{+/mid}$, thus potentially constituting the precursor cells for lung interstitial macrophages, alveolar macrophages, and dendritic macrophages. It is known that these cells terminally differentiate into macrophages or dendritic cells within the lungs and that this process depends greatly upon the local cytokine environment, particularly GM-CSF (12).

Based upon our data, it is possible that two separate pathways of differentiation may occur. In the first, $CD11b^{-}/CD11c^{+/high}$ alveolar macrophages or immature dendritic cells located in the alveolar spaces may be activated by the presence of the infection and increase their expression of CD11b, becoming $CD11b^{+/high}/CD11c^{+/high}$ activated macrophages or differentiated dendritic cells. The second pathway of differentiation that may occur within the $CD11b^{+/mid}/CD11c^{+/mid}$ population is up-regulation of CD11b and CD11c markers, becoming the differentiated $CD11b^{+/high}/CD11c^{+/high}$ dendritic cells observed in region R6.

The data also demonstrate that costaining with CD11b and CD11c allows a more precise definition of the cell subsets. To date, several reports (13–16) have used $CD11c^{+}$ staining as the sole marker to identify dendritic cells without taking into account that this marker is also expressed on alveolar macrophages. In addition to these latter cells, we found that the BAL also contained some small veiled cells that morphologically resembled immature dendritic cells, consistent with previous reports (17, 18). Moreover, whereas lymphocytes clustered as a dense region in the FSC^{low}/SSC^{low} (R2) area, this region also contained ~23% of

Table III. *Percentage of lung cells in each region of the CD11b/CD11c dot plot from naive, early, or chronic stage of murine pulmonary infection with* M. tuberculosis[a]

Infection Stage	R5 $CD11b^{-}/CD11c^{+/high}$ Alveolar Macrophages	R6 $CD11b^{+/high}/CD11c^{+/high}$ Dendritic Cells	R7 $CD11b^{+/mid}/CD11c^{+/mid}$ Monocytes/Small Macrophages	R8 $CD11b^{+/high}/CD11c^{-}$ Monocytes/Small Macrophages	R9 $CD11b^{+/high}/CD11c^{-}$ Granulocytes (Neutrophils)
Naive	20	1	3	4	4
Early	16	7	6	6	4
Chronic	6	4	6	8	14

[a] Lung cells from mice in naive ($n = 4$) and early ($n = 4$) or chronic ($n = 4$) stage of infection after pulmonary challenge with *M. tuberculosis* were stained for CD11b and CD11c expression. The percentage of cells in each region of the CD11b/CD11c dot plot was determined. These results are from one representative experiment at each time point. Four experiments were done for early phase of infection (21 days) and two experiments were done for the chronic phase of infection (240 days). Each experiment was compared with naive mice of similar age.

cells that stained $CD11b^+$ and in addition for F4/80, a marker of monocyte/macrophage lineage cells (19).

Additional characterization of cells in these regions using expression of costimulatory Ags (CD80 and CD86), CD40, and class II MHC Ags, together with morphological characterization of sorted cell populations showed that $CD11b^-/CD11c^{+/high}$ (R5) cells were a mixture of alveolar macrophages and early immature dendritic cells, whereas $CD11b^+/CD11c^{+/high}$ (R6) cells were mainly differentiated dendritic cells and some activated macrophages. As discussed above, we speculate that alveolar macrophages or immature dendritic cells contained in the R5 gate may differentiate into activated macrophages or dendritic cells located in the R6 region. In fact, sorting of $CD11b^-/CD11c^{+/high}$ cells from both the lung digests and BAL showed the morphology of alveolar macrophages, and treatment of these cells with LPS triggered them to change their phenotype to $CD11b^{+/mid}/CD11c^{+/high}$ (data not shown).

Cells in the R6 region expressed high levels of CD80, CD86, CD40, and class II MHC and had the typical morphology of differentiated dendritic cells. After infection, a significant increase in CD40 expression occurred, and this could be observed as early as day 7. Notably, however, up-regulation of class II MHC was observed, but not to the extent that might have been anticipated (Table II and Fig. 6). This may reflect some degree of inhibition of Ag presentation caused by the bacterium itself or mycobacteria Ags, as several laboratories have recently noted (20–23).

As verified by cell sorting, the R9 region was represented by neutrophils. Using conventional microscopy it is usually difficult to find neutrophils in the very early stages of the lung infection, but the data shown here verify that this population of cells does indeed enter the lungs early. As noted elsewhere (11), depletion of these cells seems to cause a transient drop in resistance early in the infection.

Based upon these observations, we also examined macrophage populations harvested from mice well into the chronic or latent phase of the infection. What was notable that increased expression of markers associated with activation and Ag presentation was not apparent on the macrophage subsets present at this later stage of the infection. The status of events during this stage of the disease is still poorly understood, both at the bacterial and host response levels. The data imply that fresh monocytes are still entering the granulomatous lesions at this later time, but they may not be differentiating further. Ag presentation appears completely shut down, which may simply reflect the fact that Ag is not being produced by bacteria because they are in a latent state, or that Ag presentation is being actively interfered. The latter is supported by our results in which APCs in the lung during the chronic stage of *M. tuberculosis* infection did not have the activated phenotype required to present Ag to T cells. These data are in accordance with previous reports indicating that cultured cells infected with *M. tuberculosis* resulted in defective Ag processing because of several factors, from down-regulation of cell surface expression of MHC class II Ags (21) and defective trafficking of immature class II molecules (20, 24, 25), to interferences of *M. tuberculosis* with the cellular transcriptional pathways that are activated by IFN-γ (26), to specific action of lipoproteins from the mycobacterial lysate with Ag processing (20). In addition, it is also known that the local cytokine environment at this time includes cytokines such as IL-6, IL-10, and TGFβ, which are down-regulatory (27–29). As we have recently suggested, accumulation of IL-10 may directly trigger reactivation disease (30).

In summary, flow cytometric analysis centering on the identification of the levels of expression of the CD11b and CD11c markers can be used to distinguish between subsets of macrophages in the lungs and their changes with time after *M. tuberculosis* infection. This information should facilitate further investigations into both the physiology and contributions of these populations to the expression of host immunity in the lungs.

Acknowledgments

We thank Dr. Angelo Izzo for critically reading the manuscript.

References

1. World Health Organization. 2002. Global tuberculosis control: surveillance, planning, financing. In *WHO Report 2002*. Communicable Diseases, World Health Organization, Geneva.
2. Steinman, R. M. 1991. The dendritic cell system and its role in immunogenicity. *Annu. Rev. Immunol. 9:271*.
3. Bancherau, J., and R. Steinman. 1998. Dendritic cells and the control of immunity. Nature *392:245*.
4. Rhoades, E., A. Frank, and I. Orme. 1997. Progression of chronic pulmonary tuberculosis in mice aerogenically infected with virulent *Mycobacterium tuberculosis. Tuber. Lung Dis. 78:75*.
5. Cooper, A. M., D. K. Dalton, T. A. Stewart, J. P. Griffin, D. G. Russell, and I. M. Orme. 1993. Disseminated tuberculosis in interferon γ gene-disrupted mice. *J. Exp. Med. 178:2243*.
6. Flynn, J. L., J. Chan, K. J. Triebold, D. K. Dalton, T. A. Stewart, and B. R. Bloom. 1993. An essential role for interferon γ in resistance to *Mycobacterium tuberculosis* infection. *J. Exp. Med. 178:2249*.
7. Orme, I. M. 1998. The immunopathogenesis of tuberculosis: a new working hypothesis. *Trends Microbiol. 6:94*.
8. Orme, I. M., and A. M. Cooper. 1999. Cytokine/chemokine cascades in immunity to tuberculosis. *Immunol. Today 20:307*.
9. Roberts, A. D., A. M. Cooper, J. T. Beslisle, J. Turner, M. Gonzalez-Juarrero, and I. M. Orme. 2002. Murine model of tuberculosis. In *Methods in Microbiology*, Vol. 32. S. H. E. Kaufmann and D. Kabelitz, eds. Elsevier Sciences, New York, p. 433.
10. Gonzalez-Juarrero, M., O. C. Turner, J. Turner, P. Marietta, J. V. Brooks, and I. M. Orme. 2001. Temporal and spatial arrangement of lymphocytes within lung granulomas induced by aerosol infection with *Mycobacterium tuberculosis. Infect. Immun. 69:1722*.
11. Pedrosa, J., B. M. Saunders, R. Appelberg, I. M. Orme, M. T. Silva, and A. M. Cooper. 2000. Neutrophils play a protective, non-phagocytic, role in systemic *Mycobacterium tuberculosis* infection of mice. *Infect. Immun. 68:577*.
12. Shitaba, Y., P.-Y. Berclaz, Z. C. Chroneos, M. Yoshida, J. A. Whitsett, and B. C. Trapnell. 2001. GM-CSF regulates alveolar macrophage differentiation and innate immunity in the lung through PU.1. *Immunity 15:557*.
13. Peters, W., H. M. Scott, H. F. Chambers, J. Flynn, I. F. Charo, and J. D. Ernst. 2001. Chemokine receptor 2 serves an early and essential role in resistance to *Mycobacterium tuberculosis. Proc. Natl. Acad. Sci. USA 98:7958*.
14. Jiao, X., R. Lo-Man, P. Guermonpez, L. Fiette, E. Deriaud, S. Burgaud, B. Gicquel, N. Winter, and C. Leclerc. 2002. Dendritic cells are host cells for mycobacteria in vivo that trigger innate and acquired immunity. *J. Immunol. 168:1294*.
15. Gonzalez-Juarrero, M., and I. M. Orme. 2001. Characterization of murine lung dendritic cells infected with *Mycobacterium tuberculosis. Infect. Immun. 69:1127*.
16. Tailleux, L., O. Schwartz, J.-L. Hermann, E. Pivert, M. Jackson, A. Amara, L. Legres, D. Dreher, L. P. Nicod, J. C. Gluckman, et al. 2003. DC-SIGN is the major *Mycobacterium tuberculosis* receptor on human dendritic cells. *J. Exp. Immunol. 197:1*.
17. Holt, P. G., and M. Schon-Hegrad. 1987. Localization of T cells, macrophages and dendritic cells in respiratory tract tissue: implications for immune functions studies. *Immunology 62:349*.
18. Casarolo, M., J. Bernandin, C. Saltin, V. Ferraus, and R. Crystal. 1988. Accumulation of Langerhan's cells on the epithelial surface of the upper respiratory tract in normal subjects in association with cigarette smoking. *Am. Rev. Respir. Dis. 137:406*.
19. Gordon, S., S. Lawson, S. Rabinowitz, P. R. Crocker, L. Morris, and V. H. Perry. 1992. Antigen markers of macrophage differentiation in murine tissues. *Curr. Top. Microbiol. Immunol. 181:1*.
20. Noss, E., R. Pai, T. Sallati, J. Radolf, J. Belisle, D. Golenbock, W. Boom, and C. Harding. 2001. Toll-like receptor 2-dependent inhibition of macrophage class II MHC expression and antigen processing by 19-kDa lipoprotein of *Mycobacterium tuberculosis. J. Immunol. 167:910*.
21. Harding, C. V., L. Ramachandra, and M. J. Wick. 2003. Interaction of bacteria with antigen presenting cells: influences on antigen presentation and antibacterial immunity. *Curr. Opin. Immunol. 15:112*.

22. Ramachandra, L., E. Noss, W. H. Boom, and C. V. Harding. 2001. Processing of *Mycobacterium tuberculosis* antigen 85B involves intraphagosomal formation of peptide-major histocompatibility class II complexes and is inhibited by live bacilli that decrease phagosome maturation. *J. Exp. Med. 194:1421.*
23. Clemens, D., and M. Horwitz. 1995. Characterization of the *Mycobacterium tuberculosis* phagosome and evidence that phagosomal maturation is inhibited. *J. Exp. Med. 181:257*.
24. Hmama, Z., R. Gabathuler, W. A. Jefferies, G. de Jong, and N. E. Reiner. 1998. Attenuation of HLA-DR expression by mononuclear phagocytes infected with *Mycobacerium tuberculosis* is related to intracellular sequestration of immature class II heterodimers. *J. Immunol. 161:4882.*
25. Wojciechowski, W., J. DeSanctis, E. Skamene, and D. Radzioch. 1999. Attenuation of MHC class II expression in macrophages infected with *Mycobacterium bovis* bacillus Calmette-Geurin involves class II transactivator and depends on the *Nramp*1 gene. *J. Immunol. 163:2688.*
26. Ting, L.-M., A. C. Kim, A. Cattamanchi, and J. D. Ernst. 1999. Mycobacterium tuberculosis inhibits IFN-γ transcriptional responses without inhibiting activation of STAT1. *J. Immunol. 163:3898.*
27. vanHeyningen, T. K., H. L. Collins, and D. G. Russell. 1997. IL-6 produced by macrophages infected with *Mycobacterium* species suppresses T cell responses. *J. Immunol. 158:330.*
28. Giancomini, E., E. Iona, L. Ferroni, M. Mienttinen, L. Fattorini, G. Orefici, I. Julkenen, and E. M. Coccia. 2001. Infection of human macrophages and dendritic cells with *Mycobacterium tuberculosis* induces a differential cytokine gene expression that modulates T cell response. *J. Immunol. 166:7033.*
29. Toossi, Z., P. Gogate, H. Shiratsuchi, T. Young, and J. J. Ellner. 1995. Enhanced production of TGF-β by blood monocytes from patients with active tuberculosis and presence of TGF-β in tuberculosis granulomotous lung lesions. *J. Immunol. 154:465*.
30. Turner, J., M. Gonzalez-Juarrero, D. L. Ellis, R. J. Basaraba, A. Kipnis, I. M. Orme, and A. M. Cooper. 2002. In vivo IL-10 production reactivates chronic pulmonary tuberculosis in C57BL/6 mice. *J. Immunol. 169:6343.*